

## Phase stabilization in cinnarizine complexes using X-ray profile analysis

G NAGENDRAPPA, S SUBRAMANYA RAJ URS, M S MADHAVA\* and R SOMASHEKAR\*

Department of Studies in Chemistry; \*Department of Studies in Physics, University of Mysore, Mysore 570 006, India

MS received 12 April 2000; revised 18 December 2000

**Abstract.** Characterization of cobalt(II), cadmium(II), copper(II) and tin(II) cinnarizine complexes have been carried out using conductivity, electronic spectra, infrared, nmr, thermogravimetric and X-ray analyses to establish the nature of phase stabilization in these materials. Also, the intrinsic strain components present in these materials during the formation have been computed using wide-angle X-ray scattering analysis. The variation of the crystallite shape ellipsoid in these materials has been discussed on the basis of Hosemann's paracrystalline model.

**Keywords.** Crystallite shape; strain; cinnarizine; WAXS.

**PACS Nos** 61.10-i; 61.66.Hq; 61.72.-y; 61.72.Qq

### 1. Introduction

Cobalt(II), copper(II), cadmium(II) and tin(II) anionic complexes associated with organic cations are well established [1–5] and some of the ion-association compounds are finding analytical applications [1,6]. Cinnarizine is a drug used as a calcium blocker. It is a piperazine derivative, piperazine being used to prepare ion-association complexes [1,7] and it also contains an alkene group which offers an interesting feature in understanding the structure and bonding [8] of its cation associated metal complexes. Therefore, an attempt has been made to prepare cinnarizinium divalent cation associated tetrachlorometallate(II),  $MCl_4^{-2}$  where  $M = Co(1), Cu(2), Cd(3)$  and  $Sn(4)$  complex anions and the complexes are being characterized for their composition, structure and geometry via various physico-chemical methods. On the basis of Hosemann's paracrystalline model [9–12] and using X-ray data we present here a method for identifying the most stabilized phase among the different metal complexes and this fact is further justified by the thermal results.

### 2. Preparation of the complexes

All the four complexes were prepared by a general method of mixing 0.1 M 25 ml ethanolic solution of respective metal chlorides with 0.122 M 25 ml alcoholic solution of cinnarizine

hydrochloride, then pH of the solution was adjusted to about 4–5 with 2 M hydrochloric acid. The resulting solution was slowly evaporated to about 10 ml on a water bath. The concentrated solution was kept at room temperature for about 20–24 h. During this period crystalline blue(1), or yellow(2) or colourless(3 and 4) complex was obtained. The complex was separated by filtration and dried in a desiccator over anhydrous silica gel yield and melting point were determined, (1) 1.40 g, 80%, m.p. 206–210 °C, (2) 1.20 g, 78%, m.p. 175–180 °C, (3) 1.30 g, 68%, m.p. 179–182 °C and (4) 1.35 g, 70%, m.p. 215–220 °C. Later the complexes were analysed for the elements (RSIC, Lucknow) and following data is obtained, found and (calculated) in per centage as follows:

(1) Co: 10.28 and (10.31) C: 54.70 and (54.66) N: 4.88 and (4.90) Cl: 25.10 and (24.82)

(2) Cu: 10.90 and (11.03) C: 54.10 and (54.22) N: 4.80 and (4.86) Cl: 24.50 and (24.62)

(3) Cd: 18.00 and (17.99) C: 49.80 and (49.98) N: 4.20 and (4.48) Cl: 21.90 and (22.47)

(4) Sn: 18.90 and (18.81) C: 49.20 and (49.48) N: 4.21 and (4.43) Cl: 21.90 and (22.47)

Conductivities were measured for  $10^{-3}$  M solutions of complexes in acetonitrile employing a Toshniwal conductivity bridge provided with a diptype conductivity cell. The conductivities were 86.24, 95.16, 80.34 and 81.14  $\text{ohm}^{-1} \text{cm}^2 \text{mol}^{-1}$  respectively for 1, 2, 3 and 4 complexes.

IR spectra of complexes and cinnarizine hydrochloride were recorded as KBr pellets employing Bruker 1F355, IR spectrum of copper(II) complex is shown in figure 1 and main peaks observed in the spectra were as follows: 3014, 2941, 2671, 2580, 1492, 1447, 1421, 1315, 1184, 1076, 1020, 977, 921, 758, 703, 648, 615, 583, 487, and 374  $\text{cm}^{-1}$ .

NMR spectra of Cd(II), Sn(II) complexes and cinnarizine hydrochloride were recorded using TMS as internal standard employing Hitachi Perkin Elmer 60 MHz NMR spectrometer and the signal  $\delta$  ppm observed were as follows: 7.0–7.6 (Ar-H), 6.3–6.8 ( $-\text{CH}=\text{CH}_2$ ), 4.2–4.6 ( $\text{CH}=\text{CH}_2$ ), 3.2–3.7, 2.0–3.0 ( $-\text{NH}$ ).

Magnetic susceptibility of the complexes were determined by Gouy method employing mercury tetrathiocyanato cobaltate(II) as a calibrant, after applying diamagnetic correction,

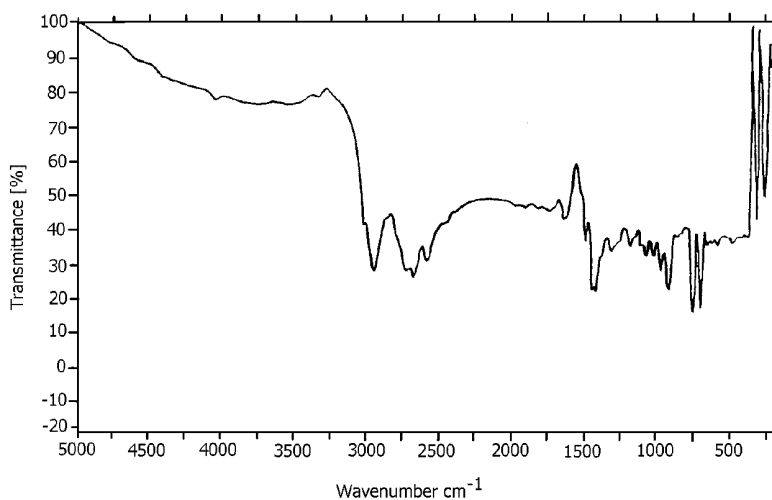
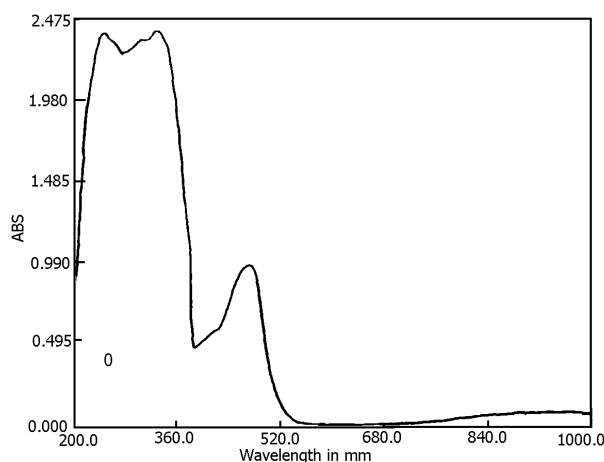
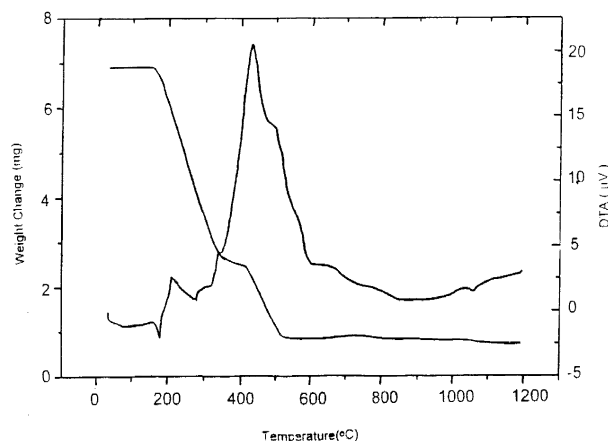


Figure 1. IR spectrum of copper(II) complex.



**Figure 2.** Absorption spectrum of  $[C_{26}H_{30}N_2][CuCl_4]$ .



**Figure 3.** TGA and DTA of  $[C_{26}H_{30}N_2][CuCl_4]$ .

the magnetic moment 4.65 BM and 1.99 BM were obtained for cobalt(II) and copper(II) complexes and cadmium(II) and tin(II) complexes were found to be diamagnetic.

UV-visible absorption spectra of complexes and that of cinnarizine hydrochloride were recorded for their solution in acetonitrile employing JASCO 610 UVdec double beam spectrophotometer equipped with 1 cm silica cells. The absorption spectrum of copper(II) complex is shown in figure 2. The absorption bands observed were in the following regions:  $15218\text{--}21786\text{ cm}^{-1}$ ,  $11074\text{--}23809\text{ cm}^{-1}$ ,  $14508\text{--}22450\text{ cm}^{-1}$ ,  $13750\text{--}21640\text{ cm}^{-1}$  and  $34602\text{--}42016\text{ cm}^{-1}$  for Co(II), Cu(II), Cd(II), Sn(II) complexes and cinnarizine hydrochloride.

Thermograms (TGA) of the complexes were recorded employing rheometric scientific STA-1500 thermal analyser at a heating rate of  $10^\circ\text{C}$  per min under nitrogen/oxygen atmosphere and that of copper(II) complex is given in figure 3.

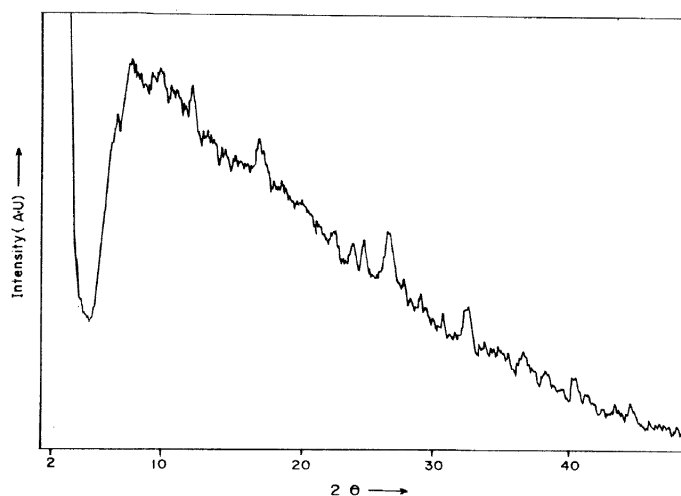


Figure 4. XRD pattern of copper(II) complex.

### 2.1 X-ray studies

X-ray powder pattern recordings of all the samples were carried out with JEOL, Japan XRD, and the wavelength ( $\lambda$ ) of the radiation used is 1.934 Å. The XRD pattern of the copper(II) complex is shown in figure 4. The pattern collected was corrected for Lorentz polarization and also for instrumental broadening using Stokes [13] deconvolution method.

A trial and error method suggested by De Wolff [14] was used to identify the reflections of all the samples and cell parameters with identified ( $hkl$ ) reflection and are given in table 1 for all the samples studied here.

The X-ray profiles for each of the observed Bragg reflections were employed for estimation of the crystal imperfection parameters, using recently reported method [15] where one-dimensional paracrystalline model of Hosemann's [12,16] which takes into account both parameters: crystal size and lattice strain while estimating the broadening of a profile has been employed. It is to be observed here that Scherrer equation does not consider the strain present in the sample, hence leading to the over estimation of crystal size. For our analysis, we have considered reflections which are well separated and have least overlapping with the neighbouring reflections.

Here  $N$  is the number of unit cells counted in a direction perpendicular to the ( $hkl$ ) Bragg plane and  $g$  is the lattice strain which arises due to disorder of II kind. For various values of  $N$  and  $g$ , and employing one-dimensional Hosemann's model we can simulate an X-ray profile using the following equations [15,17]

$$I(s) = I_{N-1}(s) + I'_N(s), \quad (1)$$

where

$$I_N(s) = 2 * \text{Re} \left[ \frac{(1 - I^{N+1})}{(1 - I)} + \frac{Iv}{d(1 - I)^2} \left\{ I^N (N(1 - I) + 1) - 1 \right\} \right]^{-1}, \quad (2)$$

**Table 1.** Microstructural parameters of cinnarizine complexes using X-ray profile analysis method.

Sample	$2\theta^\circ$	$d$ in Å	$N$	$g$ in %	$\alpha^*$	$\alpha_{av}^*$
[C <sub>26</sub> H <sub>30</sub> N <sub>2</sub> ] CoCl <sub>4</sub>	11.90	9.328	35.8	0.97	0.058	0.054
	17.23	6.457	22.8	0.91	0.043	
	32.00	3.508	39.8	0.96	0.061	
[C <sub>26</sub> H <sub>30</sub> N <sub>2</sub> ] SnCl <sub>4</sub>	11.88	9.34	21.5	0.99	0.046	0.061
	18.82	5.914	57.1	0.95	0.072	
	28.40	3.942	46.6	0.96	0.066	
[C <sub>26</sub> H <sub>30</sub> N <sub>2</sub> ] CuCl <sub>4</sub>	12.13	9.152	19.4	0.99	0.044	0.060
	17.14	6.489	50.1	0.95	0.067	
	32.42	3.464	56.8	0.92	0.069	
[C <sub>26</sub> H <sub>30</sub> N <sub>2</sub> ] CdCl <sub>4</sub>	11.59	9.572	22.4	0.99	0.047	0.060
	19.03	5.849	47.6	0.97	0.067	
	28.64	3.909	50.3	0.95	0.067	

where  $v = 2ia^2s + d$  and  $I = I_1(s) = \exp(-a^2s^2 + ids)$ ;  $a^2 = w^2/2$ . Also,

$$I'_N(s) = \frac{2a_N}{D(\pi)^{1/2}} \exp(iDs) \left[ 1 - a_N s \{ 2\mathcal{D}(a_N s) + i(\pi)^{1/2} \exp(-a_N^2 s^2) \} \right] \quad (3)$$

with  $a_N^2 = N\omega^2/2$ ,  $\omega$  is the standard deviation of the nearest neighbour probability function,  $\mathcal{D}(a_N s)$  is the Dawson's integral or the error function.  $I'_N(s)$  is the modified intensity for the probability peak centered at  $D(= Nd_{hkl})$  and is  $\sin(\theta/\lambda)$ .

The experimental profile between  $s_0$  and  $s_0 + s_0/2$  (or  $s_0$  and  $s_0 + B/2d$ , if there is a truncation of the profile  $B < 1$  and  $B = 1$ , when there is no truncation,  $d = d_{hkl}$ ) is matched with the corresponding simulated order of reflection between  $s_0$  and  $s_0/2$  (or  $s_0$  and  $s_0 + B/2d$ ) by computing the above equation for various  $N$  and  $g$  values so as to minimize the difference between calculated and experimental normalized intensity values. For minimizing we have used a SIMPLEX, a multi-dimensional algorithm [18]. Figures 5a–h show the experimental and simulated X-ray profiles for the four samples studied here.

Using this procedure, the values of  $N$  and  $g$  – the crystal size and lattice strain, obtained for X-ray reflection at various  $2\theta_p$  angles for different samples are computed and given in table 1.

### 3. Results and discussion

Data of elemental analysis and conductivity measurement of the complexes account for the general composition of the complexes (C<sub>26</sub>H<sub>30</sub>N<sub>2</sub>) (MCl<sub>4</sub>) and 1:1 electrolyte nature [19]. Magnetic moment value 4.65 and 1.99 BM respectively for cobalt(II) and copper(II) complexes coupled with colour and electron absorption spectral characteristics of cobalt(II) and copper(II) complexes will account for tetrahedral geometry for the complexes [20].

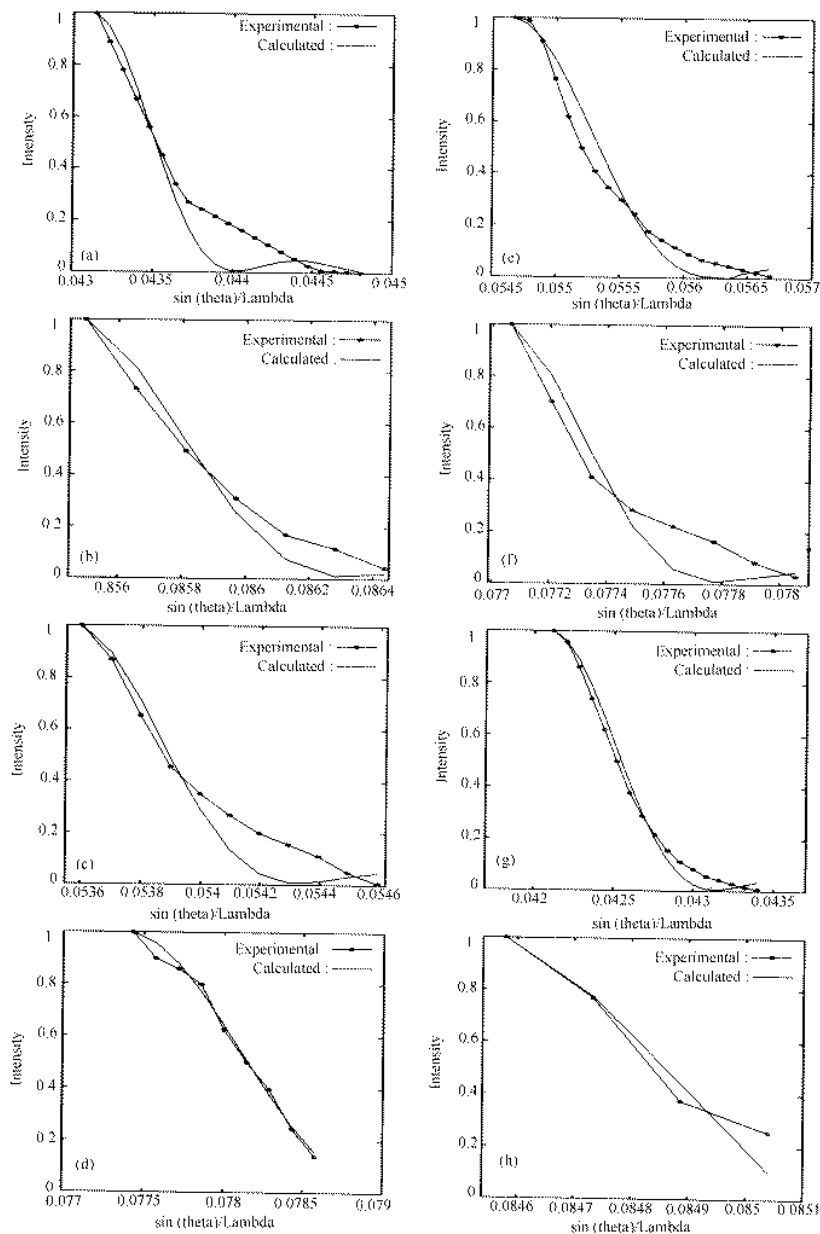


**Figure 5.** Experimental and simulated (using the parameters given in table 1 and equations mentioned in the text) X-ray profiles for the four samples studied here. (i)  $[C_{26}H_{30}N_2][CdCl_4]$  (a and b); (ii)  $[C_{26}H_{30}N_2][CoCl_4]$  (c and d); (iii)  $[C_{26}H_{30}N_2][CuCl_4]$  (e and f) and (iv)  $[C_{26}H_{30}N_2][SnCl_4]$  (g and h).

A multiplet absorption band at  $17,006.8 \text{ cm}^{-1}$  (an average at  $14,612.8+15,479.8+15,892.2 \text{ cm}^{-1}$ ) in the visible region assigned to  $4_2^A \rightarrow 4T_1(P)(\nu_3)$  electron transition, one multiplet expected in the near IR region for  $4A_2 \rightarrow 4T_1(F)(\nu_2)$   $5,414 \text{ cm}^{-1}$  is assumed and crystal field splitting and covalent parameters were calculated and found  $3102.46$ ,  $715.10 \text{ cm}^{-1}$  and  $0.6384$  respectively for  $10 Dq$ ,  $B'$  and  $\beta$  coupling the spectral data with that of the experimental magnetic moment, the spin orbit coupling constant  $\lambda'$  of the complexed cobalt(II) is calculated and found  $155.84 \text{ cm}^{-1}$  [21]. The experimental and calculated spectral parameters and magnetic moment of cobalt(II) complex agree with the established tetrachloro cobaltate(II) complexes, therefore, the tetrahedral geometry is assigned to the complex. The absorption bands at  $41,841$  and  $34,842.76 \text{ cm}^{-1}$  are similar to those observed for the UV absorption bands of cinnarizine hydrochloride, therefore, these are assigned to charge transfer transitions due to cinnarizinium ion.

The absorption bands which are characteristic of the cinnarizine hydrochloride at  $42016.8 \text{ cm}^{-1}$  and  $34602.07 \text{ cm}^{-1}$  remained same with a slight shift in all the four complexes indicating the intactness of cinnarizine cation with complexes.

The absorption spectrum of copper(II) complex (figure 2), exhibits  $d-d$  envelope at  $11,074 \text{ cm}^{-1}$  of less intensity indicating the distorted tetrahedral geometry produced by Jahn–Teller distortion and two bands at  $21413.27$  and  $31055.90 \text{ cm}^{-1}$  are assigned to charge transfer transitions  $2B_2 \rightarrow 4A_2$  and  $2B_2 \rightarrow 2E$  respectively indicating  $D_2$ ,  $\text{CuCl}_4^{2-}$ , complex ion [22]. The UV-absorption bands at  $41,666.6 \text{ cm}^{-1}$  and  $33,333.3 \text{ cm}^{-1}$  are assigned to charge transfer transitions due to cinnarizinium ion. Further the magnetic moment values confirm tetrahedral and distorted tetrahedral geometry respectively for Co(II) and Cu(II) complexes.

Absorption spectra of cadmium(II) and tin(II) complexes indicate only UV absorption bands at  $41666.6$ ,  $34246.5$ ,  $42016.8$  and  $36363.6 \text{ cm}^{-1}$  for the presence of cinnarizinium ion in both the complexes.

FT-IR spectra of cinnarizine hydrochloride regenerated from the complexes and the complexes of cinnarizine hydrochloride (with Co(II), Cu(II), Cd(II) and Sn(II)) are more or less overlapping on one another. All of them are having characteristic stretching frequencies at  $1447$ ,  $970$ , and  $700 \text{ cm}^{-1}$  which could be assigned to trans-substituted alkene group of the cinnarizine ion and those at  $3543$  and  $3426 \text{ cm}^{-1}$  are assigned to NH stretching of the organic ion indicating the structurally intact cinnarizine ion and there is no participation of alkene group in coordinating to the metal ion of any one of the four complexes.

NMR spectra of cinnarizine hydrochloride and those of cadmium(II) and tin(II) complexes are once again similar and all of them show signals at  $7.0-7.5$ ,  $2.3-3.2$  and  $6.0-6.5$  ppm which could be assigned to phenyl,  $-\text{CH}=\text{CH}_2-$ , and  $-\text{NH}$  protons respectively. The NMR spectra once again compliment the IR data accounting for the structurally intact cinnarizine cation.

### 3.1 Thermal analysis

Thermograms of all the four complexes indicate that there is no mass loss before  $420 \text{ K}$  indicating the absence of water of hydration in the complexes. The general decomposition pattern of the complexes is similar and it takes place in two stages, first one being in the temperature range of  $420$  to  $706 \text{ K}$  and the second one corresponds to the temperature range of  $710$  to  $840 \text{ K}$  and there after mass remains constant. For cobalt(II) complex the

first stage decomposition starts at 490 K and completes at 690 K. The residual mass 35.50% against the calculated 35.44% corresponds to  $H_2(CoCl_4)$ , for the copper(II) complex. The first stage starts from 437 K and completes at 708 K, where the residual mass 36.01% against the calculated 39% corresponds to  $H_2(CdCl_4)$ , 40% against the calculated 41.01% corresponds to  $H_2(CuCl_4)$ . And for the tin(II) complex the first stage begins at 425 K and closes at 675 K, where the residual mass 41% against the calculated 41.1% corresponds to  $H_2(SnCl_4)$ . For all the four complexes, the mass volatilized at the final temperature of the first stage corresponds to  $C_{26}H_{28}N_2$ .

Second stage of decomposition takes place in the temperature range 710–810 K, 710–838 K, 715–840 K and 710–820 K respectively for Co(II), Cu(II), Cd(II) and Sn(II) complexes. Final temperatures residual 13.10% against the calculated 13.12%, 13.11% against the calculated 13.81%, 21.01% against the calculated 20.55% and 21.10% against the calculated 21.34% respectively for CoO, CuO, CdO and SnO.

### 3.2 Kinetic parameters

All the four complexes exhibit a characteristic well-defined and non-overlapping decomposition pattern. Therefore, kinetic parameters have been evaluated from TGA curves using Coats and Redfern method [23], which involves plot of  $-\log[1 - (1 - \alpha)^{1-n}/T^2(1 - n)]$  against  $1/T$ . This yields a straight line with slope,  $E_a/2.303R$ , where  $\alpha$  is the fraction of complex decomposed at temperature  $T$  and  $E_a$  is the activation energy ( $KJ\ mol^{-1}$ ) and  $n$  is the order of the reaction.  $R$  is the gas constant and intercept corresponds to frequency factor,  $A$  which is related to entropy,  $\Delta S^\ddagger$  ( $J\ mol^{-1}K^{-1}$ ), by an equation (A),

$$A = KT_s/h * \exp[\Delta S^\ddagger / R],$$

where  $K$  is Boltzmann's constant,  $R$  is the gas constant,  $h$  the Planck's constant and  $T_s$  is the peak temperature taken from DTG. Graph was plotted in each case of the complex assuming the order  $n = 1/2$  and yielded good straight lines for first as well as second stages for all the four complexes. Details are indicated in table 2. The negative values were obtained for first second stages for all the four complexes. This indicate that the complexes are having more ordered structures than the reactants and that the rate of decompositions is slower than the normal [24–28].

### 3.3 X-ray analysis

It is evident from table 1 that there are significant changes in the values of micro crystalline parameters  $N$  and  $g$  corresponding to the same Bragg reflection of different samples. As there is an interplane between these two crystal imperfection parameters, the changes are at best described by a parameter called enthalpy ( $\alpha^* = \langle N \rangle^{1/2}g$ ) [16] which is described as the energy needed for the net plane structure is appreciably controlled by the extent of lattice disorder of type II, quantified in terms of the  $g$  value. A comparison of average  $\alpha^*$  values for different metal complexes indicate that for 'Co' complex, it is minimum and maximum for Cu. As per Hosemann,  $\alpha^*$  value for a perfect crystal is less than 0.15. The standard deviation for  $N$ ,  $g$  and  $\alpha^*$  is less than 5% of the mean value.

**Table 2.** Activation energy, frequency factor and entropy for  $[C_{26}H_{30}N_2][CoCl_4]$ ,  $[C_{26}H_{30}N_2][CuCl_4]$ ,  $[C_{26}H_{30}N_2][CdCl_4]$ , and  $[C_{26}H_{30}N_2][SnCl_4]$ .

Sample	Stage of thermal degradation	Temp. range (K)	Parameters	DTG Max. Temp. in K	Coats and Redfern
1(I) $[C_{26}H_{30}N_2][CoCl_4] \rightarrow [CoCl_4]H_2 + [C_{26}H_{28}N_2]$	I	490–690	$E_a$	515.8	7.65
			$A$		5.285
			$\Delta S$		–277.8
1(II) $[CoCl_4]H_2 \rightarrow CoO + 2HCl \uparrow + Cl_2 \uparrow$	II	710–801	$E_a$	713	9.24
			$A$		5.595
			$\Delta S$		–280.5
2(I) $[C_{26}H_{30}N_2][CuCl_4] \rightarrow [CuCl_4]H_2 + [C_{26}H_{28}N_2]$	I	437–708	$E_a$	487	8.05
			$A$		5.410
			$\Delta S$		–277.1
2(II) $[CuCl_4]H_2 \rightarrow CuO + 2HCl \uparrow + Cl_2 \uparrow$	II	710–838	$E_a$	723	11.50
			$A$		5.535
			$\Delta S$		–280.7
3(I) $[C_{26}H_{30}N_2][CdCl_4] \rightarrow [CdCl_4]H_2 + [C_{26}H_{28}N_2]$	I	420–706	$E_a$	491	8.58
			$A$		5.460
			$\Delta S$		–277.1
3(II) $[CdCl_4]H_2 \rightarrow CdO + 2HCl \uparrow + Cl_2 \uparrow$	II	715–840	$E_a$	721	9.24
			$A$		5.570
			$\Delta S$		–280.6
4(I) $[C_{26}H_{30}N_2][SnCl_4] \rightarrow [SnCl_4]H_2 + [C_{26}H_{28}N_2]$	I	435–710	$E_a$	493.0	8.46
			$A$		5.484
			$\Delta S$		–277.1
4(II) $[SnCl_4]H_2 \rightarrow SnO + 2HCl \uparrow + Cl_2 \uparrow$	II	710–820	$E_a$	715	11.56
			$A$		5.569
			$\Delta S$		–280.5

This numerical result indicates that Co complex is more phase stabilized than other samples [29]. This fact is further justified by table 1 where the percentage of metal (Co) is lowest and the other elements are relatively high when compared to all other samples (C, Cl, N). From thermal analysis, it follows that the activation energy is also lowest for ‘Co’ complex, which indicates that phase is stabilized with ‘Co’ metal rather than other metal.

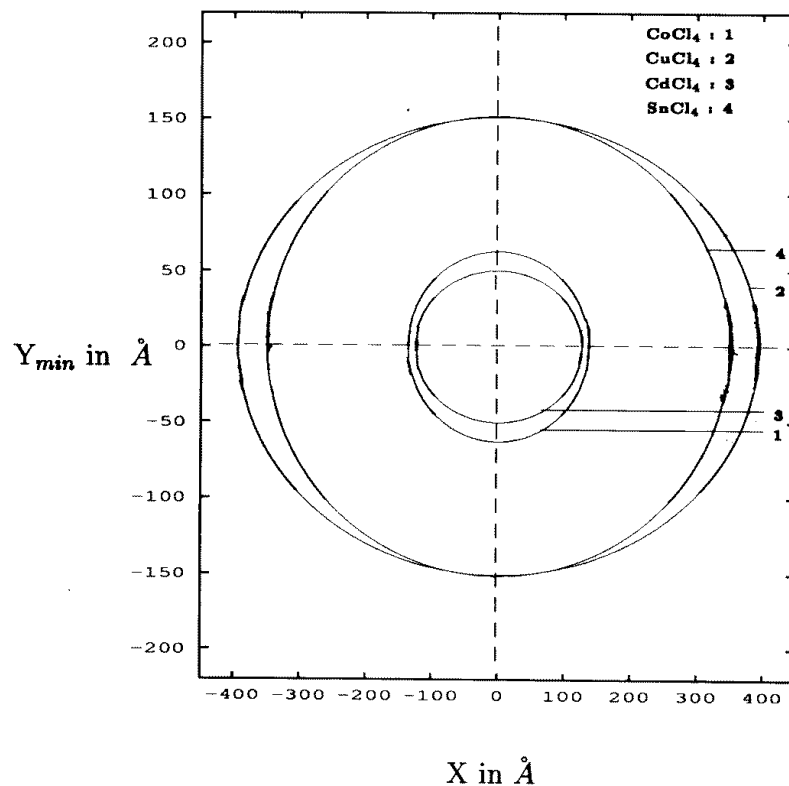
Further, for a better perspective of the results, we can project the crystal size values to a common plane using the equation [30]

$$(2/D_{hkl})^2 = (\cos \phi/X)^2 + (\sin \phi/Y)^2, \quad (4)$$

where  $\phi$  is the angle between the  $hkl$  planes which can be computed using the cell parameters and the relation given in the ‘International Crystallographic Tables (Vol I, II, III)’. The results are given in table 3. Then the variation of the shape of the crystallite ellipsoid in different metal complexes is shown in figure 6. This clearly indicates the changes in the volume of the crystalline region due to the presence of different metal complex ions.

**Table 3.** Ellipticity parameters for cinnarizine complexes.

Sample	$X$ in Å	$Y_{min}$ in Å	$Y/X$	Volume in Å <sup>3</sup>
[C <sub>26</sub> H <sub>30</sub> N <sub>2</sub> ] CoCl <sub>4</sub>	137.27	62.77	0.426	$8.63 \times 10^6$
[C <sub>26</sub> H <sub>30</sub> N <sub>2</sub> ] CuCl <sub>4</sub>	393.52	150.86	0.77	$45.8 \times 10^6$
[C <sub>26</sub> H <sub>30</sub> N <sub>2</sub> ] CdCl <sub>4</sub>	126.70	50.16	0.234	$8.33 \times 10^6$
[C <sub>26</sub> H <sub>30</sub> N <sub>2</sub> ] SnCl <sub>4</sub>	349.52	151.52	0.825	$40.25 \times 10^6$

**Figure 6.** Variation of crystallite shape ellipsoid in different metal cinnarizine complexes.

#### 4. Conclusion

Using X-ray profile analysis, and in conjunction with thermal analysis, we have established quantitatively that metal complex with 'Co' as a metal is more stabilized than other metal complexes studied here. Definite changes in the shape of crystallite ellipsoid due to

the presence of different metal ions has been presented here. These changes occur due to cinnarizinium ion in the complex acting as a cation thereby stabilizing the complex anion  $[MCl_4]^{2-}$ ,  $M = Co, Cu, Cd$  and  $Sn$ . These facts are further justified by IR and NMR studies which confirm that there is no participation of alkene group in complexation with metal ions. Further, elemental analysis, conductivity, electronic and magnetic data indicate tetrahedral geometry for  $Co(II)$ ,  $Cd(II)$  and  $Sn(II)$  metal ions and distorted tetrahedral geometry for  $Cu(II)$  metal ion complexes.

## 5. Acknowledgement

The authors (GN) and (SS) would like to thank P R Vasudeva Rao and G Periaswamy for their help in recording thermograms and also for their encouragement. They also thank U D Prahallad, USIC, University of Mysore for assisting in the XRD recordings. Author (RS) thanks JSPS, Japan for a visiting fellowship.

## References

- [1] S M Hassan Saad, B Abbas Ala and A F Elmosallamy Mohamed, *Mikrochim. Acta*, **128(1-2)**, 69–74 (1998)
- [2] G Nagendrappa, Studies on ion-pair complexes of *d*-block elements, Ph. D. thesis (Mysore University, 1994) pp. 70
- [3] Robert C Lucas and Liu Shuang, *Can. J. Chem.* **74**, 2340 (1996)
- [4] Jose S Casas, Eduardo E Cartellano, Maria D Couce, Augustin Sanchez, Jose Sordo, Jose M Varela and Julio Zukerman Scrtpector, *Inorg. Chem.* **34**, 2430 (1995)
- [5] F A Cotton and Geoffrey Wilkinson, *Advanced inorganic chemistry* (John Wiley and Sons, New York, 1988) p. 303
- [6] Koichi Yamamoto, *Talanta* **36(5)**, 561 (1989)  
Toshio Takayanagi, Eiko Wada and Shoji Motomizu, *Analyst* **122**, 57 (1997)  
Andrew Mills and Mark Thomas, *Analyst* **122**, 63 (1997)  
Jose Anchieta Gomes Neto, Bergamint H, Elias Ayres G Zagatto and Francisco J Krug, *Analytica Chimica Acta* **308**, 439 (1995)  
J Forguson, *J. Chem. Phys.* **32(2)**, 528 (1960)
- [7] Saleh G A and Askal H F, *Pharmazie* **45(3)**, 220 (1990)  
Margaret Ann James, Jason A C Clyburne, Anthony Linden, Bruce D James, John Liesegang and Vilmazuzich, *Can. J. Chem.* **74**, 1490 (1996)
- [8] George Darren S A, McDonald Robert and Cowie Martin, *Can. J. Chem.* **74**, 2289 (1996); *Chromatographic Sci. Series*, Complexation Chromatography edited by D Cagniant (Marcel Dekker Inc., New York, 1992) vol. 57, p. 152
- [9] B E Warren, *X-ray diffraction* (Addison-Wesley, Reading MA, 1969) p. 264
- [10] B E Warren, *Prog. Metal Phys.* **8**, 146 (1959)
- [11] B K Vainshtein, *Diffraction of X-rays by chain molecules* (Elsevier Publishing Co. Amsterdam, London and New York, 1996)
- [12] R Hosemann, *Progr. Coll. Poly. Sci.* **77**, 15 (1988)
- [13] A R Stokes, *Acta. Cryst.* **8**, 27 (1955)
- [14] P M De Wolff, *J. Appl. Cryst.* **1**, 108 (1968)
- [15] R Somashekar and H Somashekarappa, *J. Appl. Cryst.* **30**, 147 (1997)

- [16] R Hosemann and S N Bagchi, *Direct analysis of diffraction by matter* (Amsterdam, North Holland, 1962)
- [17] Mark Silver, Theoretical models for the wide angle X-ray diffraction pattern of a single crystal using paracrystalline probability statistics, M.Sc. thesis (UMIST, UK, 1988)
- [18] W Press, B P Flannery, S Teuklosky and W T Vettering, *Numerical recipes* (Cambridge University Press, UK, 1986) p. 83
- [19] E A Pisarev and Shevchenko Yu N, *Russian J. Inorg.* **30(5)**, 671 (1985)  
M A Bennett, R J H Clark and A D J Goodwin, *Inorg. Chem.* **6(9)**, 1625 (1967)
- [20] D M L Goodgame, M Goodgame and F A Cotton, *Inorg. Chem.* **1(2)**, 239 (1962)  
F A Cotton, D M L Goodgame, M Goodgame and T E Hass, *Inorg. Chem.* **1(3)**, 565 (1962)  
D Forster and D M L Goodgame, *J. Chem. Soc.* p. 2790 (1964)
- [21] A B P Lever, *Inorganic electronic spectroscopy* (Elsevier, Amsterdam, 1984) 2nd ed.
- [22] Robert C Lucas and Shuang Liu, *Can. J. Chem.* **74**, 2340 (1996)
- [23] A W Coats and J P Redfern, *Nature* **201**, 68 (1964)
- [24] S I Ali and Kownar Majid, *Indian J. Chem.* **A37**, 423 (1998)
- [25] G L Borde and J V Koleske, *J. Macromol. Sci. Chem.* **6(6)**, 1109 (1972)
- [26] D S Hubbell and S L Cooper, *J. Appl. Polym. Sci.* **21**, 3035 (1977)
- [27] V A Kargin, *J. Polym. Sci.* **C4**, 1601 (1963)
- [28] Vanquez-Torres and C A Cruz-Ramos, *J. Appl. Polym. Sci.* **54**, 1141 (1994)
- [29] K Sooryanarayana, R Somashekar and T N Guru Row, *Solid State Ionics* **104**, 319 (1997)
- [30] H Somshekarappa, R Somashekar, Vasudev Singh and S Z Ali, *Bull. Mater. Sci.* **22**, 101 (1999)